EXPERIMENTAL AND SIMULATED DEFECT DETECTION IN FIBRE REINFORCED COMPOSITE MATERIALS USING THE MICROWAVE NON-DESTRUCTIVE EVALUATION TECHNIQUE

Michael R. L. Gower[1], Maria J. Lodeiro[1], Richard M. Shaw[1], Andrew Gregory[1] and Rolf Judaschke[2]

[1]National Physical Laboratory, Materials Processing and Performance Group, Hampton Road, Teddington, Middlesex, TW11 0LW, UK
Email: michael.gower@npl.co.uk; maria.lodeiro@npl.co.uk; richard.shaw@npl.co.uk; andrew.gregory@npl.co.uk; http://www.npl.co.uk/people/michael-gower
[2]Physikalisch-Technische Bundesanstalt, Bundesallee 100, D-38116 Braunschweig, Germany
Email: rolf.judaschke@ptb.de, http://www.ptb.de/cms/ptb/fachabteilungen/abt2/fb-22/ag-222.html

Keywords: non-destructive testing, microwave, reference defect artefacts, delaminations, modelling

Abstract
The results of a study to evaluate the key parameters of the microwave inspection technique for defect detection are presented. Glass fibre-reinforced plastic (GFRP) reference defect artefacts (RDAs), in which defects are simulated artificially to provide well-defined and consistent defect sizes and locations, were used for the experimental investigations. The inspection results are compared to electromagnetic field simulations undertaken using CST Microwave Studio® modelling software. RDAs were designed and manufactured to be representative of the GFRP materials used and the defects typically occurring in diverse energy sector applications (lightweight transport, oil and gas, renewable energy). Defects within the RDAs included artificial delaminations and in-plane fibre misalignment, as well as individual and arrays of back-face drilled holes to represent discrete voids and regions of porosity, respectively. The microwave technique generally showed good detection capability for all defect types, except localised fibre misalignment, and the modelling and experimental results were in excellent agreement. The modelling showed that striations observed in the experimental scans for spatial resolution scans were due to the detection of superposed lateral standing waves within the RDAs. This work was undertaken within EMRP project ENG57 'Validated Inspection Techniques for Composites in Energy Applications (VITCEA)' [1].

1. Introduction

The excellent mechanical properties, low weight, fatigue and corrosion resistance of fibre reinforced plastic (FRP) composites gives them considerable advantages in renewable energy (wind, wave and tidal), oil and gas, and transport applications with the potential to contribute to the reduction of fossil fuel reliance, consumption and greenhouse gas emissions. However, full exploitation is hindered by the diverse range of defects and damage mechanisms that reduce the strength, stiffness and life of FRP structures. In order to follow a damage tolerant design philosophy and increase confidence in the use of FRPs, there is a need for validated non-destructive evaluation (NDE) techniques capable of detecting and sizing the many defects that directly impact FRP performance. Despite many innovations and developments in NDE, still relatively few methods are commonly used. This is mainly due to the absence of general operational procedures and perceptions that NDE is too unproven, costly or complex. There are currently no ISO NDE standards in existence that are specific to composites. Several ASTM composite NDE specific standards exist [2-4], but these tend to be focused on the

Excerpt from ISBN 978-3-00-053387-7

aerospace sector and do not address issues such as probability of detection (POD), defect size and location sensitivity needed to realise promising novel NDE techniques such as microwave inspection.

Microwave inspection relies on measuring changes in the dielectric properties of bulk non-conducting materials. The technique is relatively novel in its application to FRP composites and is ideally suited to the inspection of non-aerospace grades of GFRP that tend to have higher levels of porosity (>2%) and/or that significantly attenuate ultrasonic signals.

This paper details microwave inspection work undertaken within the EMRP ENG57 VITCEA project [1] towards; (i) evaluating the techniques for composites and their defects, as well as detection limits, (ii) operational procedures (as a pre-cursor to standardisation) and (iii) advancing theoretical simulation, taking into account material anisotropy. This would not only aid optimisation of the field application of the technique, but also supplement probability of detection (POD) methodologies using simulated data with the aim of reducing the labour costs and time requirements of experimental POD trials.

2. Experimental Methods

2.1. Design and fabrication of GFRP reference defect artefacts (RDAs)

The microwave technique was investigated using two monolithic GFRP flat panels (RDA2a and RDA5). These were designed and fabricated from Hexcel 913G (thermoset (epoxy) matrix/glass fibre) and Celstran® polyamide-12 (thermoplastic matrix/glass fibre) pre-impregnated tape materials respectively, to the design shown in Fig. 1. The finished RDAs are shown in Fig. 2.

The lay-up of RDA2a was $[0/90]_{10s}$ (cross-ply) and for RDA5 was $[0]_{16}$ (unidirectional). Both RDAs were approximately 5 mm thick. The defects incorporated within each RDA include: artificial delaminations (3, 6, 12 and 25 mm diameter), individual flat-bottomed back-face drilled holes (1, 2 and 3 mm diameter) as well as 3 x 3 hole arrays (1 mm diameter) and square-cut regions of in-plane fibre misalignment (15° to the principal fibre direction). All of the defects were included at three depth locations: near front-face, mid-thickness and near back-face.

Artificial delaminations were constructed according to the method detailed in [5-6]. These have been shown [6] to produce a well-defined acoustic barrier almost entirely preventing the transmission of ultrasound. Regions of fibre misalignment were created by replacing cut sections of a single ply with misaligned sections of equal size. Flat-bottomed holes were produced using a CNC drilling machine.

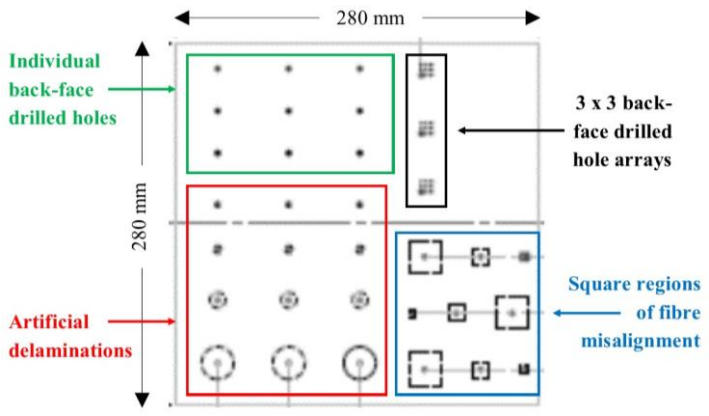

Figure 1. Generic design of GFRP monolithic, flat panel RDAs 2a and 5

Excerpt from ISBN 978-3-00-053387-7

Figure 2. Finished RDAs: RDA2a (left) and RDA5 (right)

2.2. Microwave inspection system

The inspections were performed using an Evisive Inc. microwave flat-bed scanning system, shown in Fig. 3(a). The system consists of a rigid frame mounted with a thick glass support plate. A microwave transducer is fixed to a scanning bridge fitted with x (scan direction) and y (index) linear position encoders. The system has three probe frequencies; 10.5, 24 and 34 GHz corresponding to wavelengths of ~ 30, 12.5 and 8.7 mm, respectively. Each probe consists of a transmitter diode that generates the microwaves and launches them past two sensor diodes (defined as Channels A and B), which monitor the field strength (see Fig. 3(b)), to emerge through a rectangular aperture waveguide. At each interface where there is a change in the dielectric constant in the material, the microwaves are reflected with modified amplitude and phase, interfering with the transmitted beam. The resulting signal is converted to a voltage by the sensor diodes which is then amplified and digitized. This signal is mapped and converted into greyscale images as the probe is raster scanned across the surface of the inspected component. The sensor diodes are separated by one quarter wavelength such that if one sensor detects a low or null signal, then the other sensor should detect a measurable signal, thereby increasing the sensitivity of the system.

Several experimental parameters were evaluated in this work including: (i) probe frequency, (ii) index increment and (iii) different backing materials. Both RDAs were inspected using a constant scanning speed of 100 mm/second with the probe in contact with the RDA surface at all times.

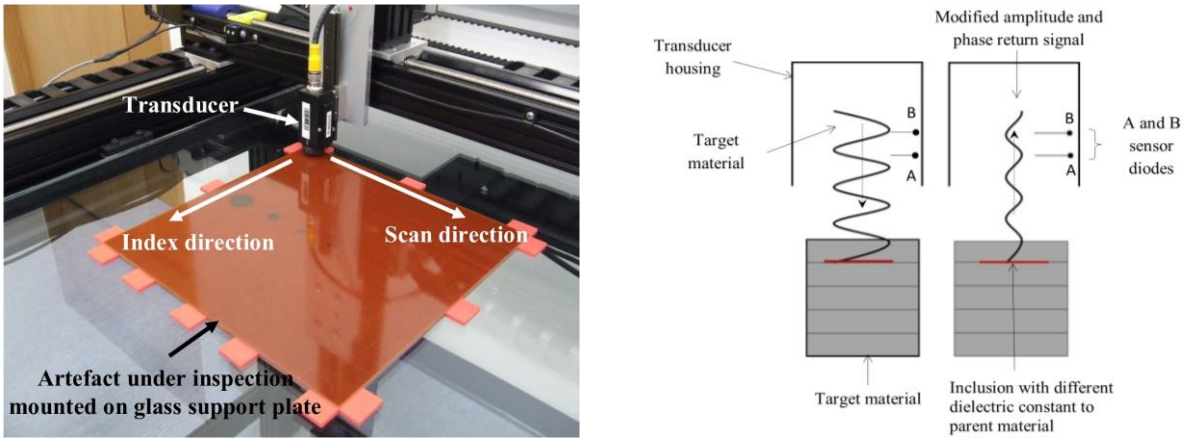

Figure 3. (a) Evisive microwave inspection system and (b) schematic of microwave transducer

Excerpt from ISBN 978-3-00-053387-7

3. Simulation of Microwave Inspection

Electromagnetic modelling simulations were undertaken which replicated both the physical set-up of the microwave inspection system used and the construction of the RDAs, enabling direct comparison with experimental inspections and theoretical predictions of defect detection.

3.1. Measurement of material dielectric properties

The complex permittivity (dielectric constant and loss) of the materials used in both RDAs were measured in the three principal directions to determine the anisotropic dielectric property datasets required for the simulations. Measurements were made using a waveguide transmission cell method and network analyser with rectangular aperture of cross-section 22.86 x 10.16 mm (Fig. 4) in accordance with ASTM D5568 [7].

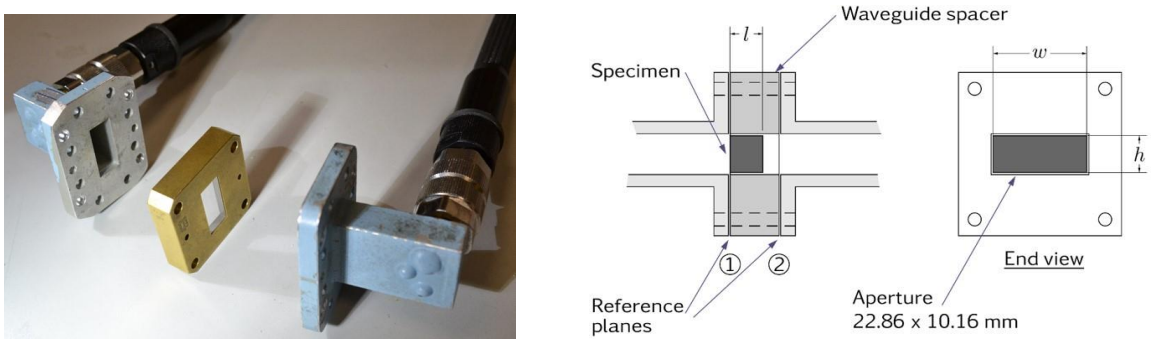

Figure 4. Transmission cell and waveguide spacer used for dielectric property measurements

The permittivity was measured for the microwave X-band between 8.2 and 12.4 GHz. In order to obtain dielectric properties at the actual inspection frequency of 24.1 GHz, the dielectric constant data at 10.5 GHz was extrapolated numerically using the Lynch formula (Eq. 1) [8], which assumes the material response is characterised by dielectric relaxation behaviour and that the loss is independent of frequency. Here $\Delta\varepsilon' = \varepsilon_1' - \varepsilon_2'$ is the real permittivity at frequencies f_1 and f_2 respectively and $\tan\delta$ is the dielectric loss where $m \approx 1.5$ for frequency independent loss.

$$\frac{\Delta\varepsilon'}{\varepsilon'} = m \tan\delta \log_{10}\left(\frac{f_2}{f_1}\right) \quad (1)$$

The average measured dielectric constant in each material direction at 10.5 GHz and values calculated for 24.1 GHz using the Lynch formula are detailed in Table 1. The dielectric constants *d1*, *d2* and *d3* were measured along the principal material axes where '1' corresponds to the principal fibre direction, '2' is the transverse in-plane direction and '3' is the through-thickness direction.

Table 1. Measured (10.5 GHz) and extrapolated (24.1 GHz) anisotropic dielectric constant data

Material	Frequency (GHz)	d1	d2	d3
Hexcel 913G	10.5	4.998	5.043	4.775
	24.1	4.947	4.996	4.731
Celstran® polyamide-12	10.5	4.323	3.773	3.765
	24.1	4.300	3.757	3.746

Excerpt from ISBN 978-3-00-053387-7

3.2. Electromagnetic modelling

Electromagnetic simulations of the microwave scanning of both RDAs were performed at 10.5, 24 and 35 GHz using electromagnetic field simulation software CST Microwave Studio® (CST). In order to compare the simulations with the inspection results obtained from the Evisive microwave scanning system, the microwave transducers were modelled in as much detail as possible. Models initially assumed material isotropy but were then adjusted to include measured dielectric data to determine how sensitive the simulations, and by inference the measurement technique, was to anisotropy.

An example of the CST simulation model is shown in Fig. 5(a). From the electromagnetic field in the waveguide reference plane, the software calculates the complex-valued input reflection coefficient. Since the RDA is nominally homogeneous, changes in the reflection coefficient as a function of the in-plane sensor position indicate a potential defect. As a compromise between spatial resolution of the simulation image and simulation time (~4 minutes per position), calculations were performed for sensor positions located on a 2 mm rectangular grid across the RDA surface. The simulated RDA was divided into 24 defect-centred sub-regions, as shown in Fig. 5(b), avoiding discretization of the full volume and minimising data storage. Fibre-misalignment defects were not considered.

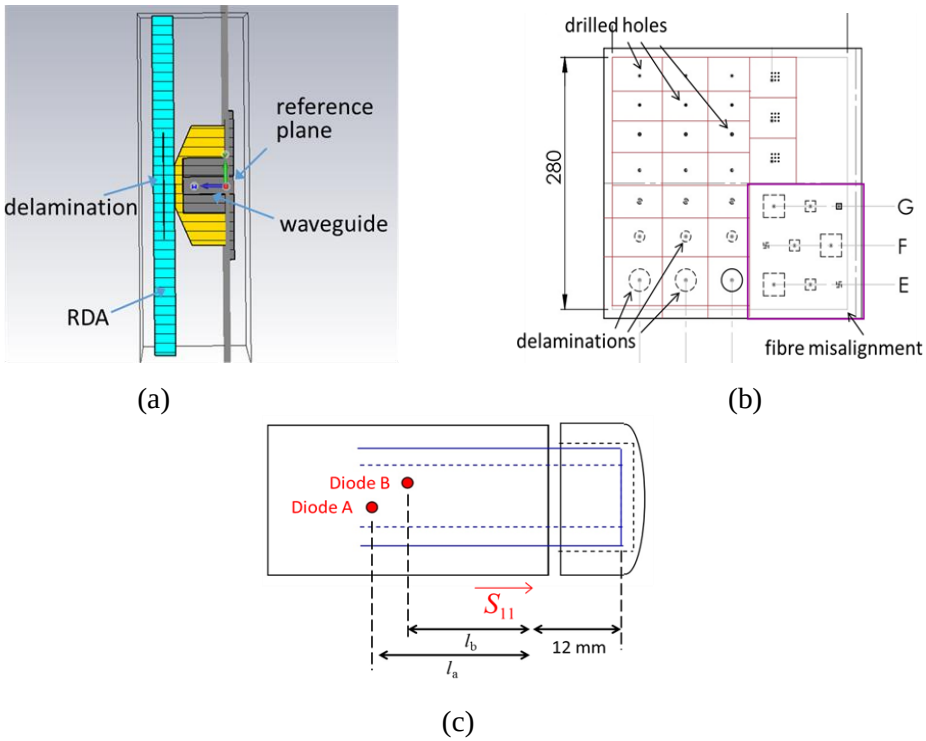

Figure 5. (a) Cross-sectional view of CST-modelled 24 GHz sensor located on RDA surface;
(b) subdivision of RDA into 24 modelling sub-regions; and
(c) transformation of S_{11} to longitudinal waveguide positions at diode A and diode B

From the simulated reflection coefficient S_{11} in the reference plane, the absolute voltage magnitude V_i (resulting from superposition of incident and reflected waves) at the detecting diode positions A and B in the microwave sensor head (detailed in Fig. 5(c)) was calculated from Eq. 2, where β and φ_{11} are the waveguide phase constant and calculated reflection coefficient phase, respectively. It is noted that the dynamic range of the simulated data has been adapted to the sensitivity of the Evisive microwave system which measures only scalar standing wave voltages.

Excerpt from ISBN 978-3-00-053387-7

$$|V(l_i)| \propto \sqrt{1+|S_{11}|^2+2|S_{11}|\cos(\varphi_{11}-2\beta l_i)} \quad (2)$$

4. Results

All microwave scan images show the 'Channel C' data (difference of Channels A and B).

4.1. Effect of transducer frequency

Figure 6 shows the inspection results for RDA2a at the different microwave frequencies. It was observed that better detection resolution was obtained with higher inspection frequencies, to be expected when one considers the relative wavelengths at each frequency. At 34 GHz, all but the smallest diameter artificial delaminations and holes were detected. In-plane fibre misalignment was not detected, due to the negligible effect on the local dielectric properties.

4.2. Effect of index increment size

Figure 7 shows the Channel C results at 34 GHz for index increments of 2 and 0.5 mm for RDA2a. Additional index increments of 4 and 8 mm were also used but are not shown. Again, the spatial resolution improves with decreasing index increment. However, at small index increments (~0.5 mm) striations were observed on the scan results which were initially thought to be an artefact of the scanning system or caused by the fibre orientation in the surface ply. However, the simulation work showed that these striations were actually due to superposition of lateral standing waves in the material, detectable at smaller index increments, and exhibited greater intensity at the RDA edges.

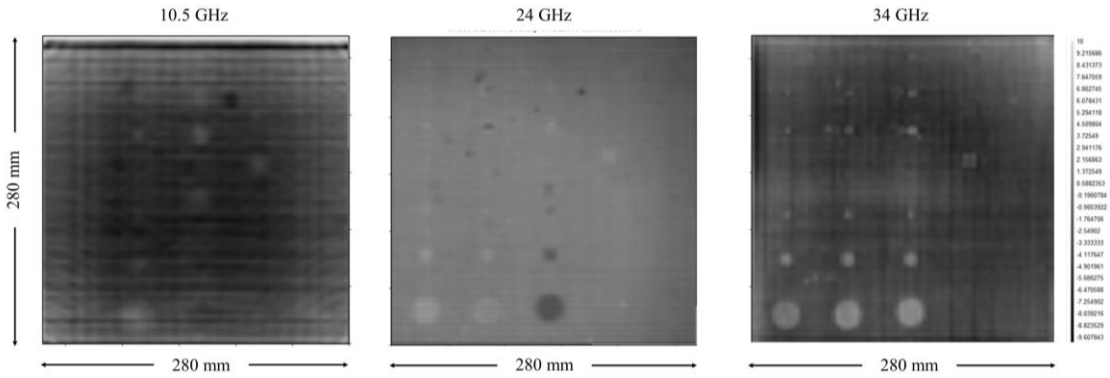

Figure 6. Inspection results for RDA2a at 10.5, 24 and 34 GHz (index increment 2 mm)

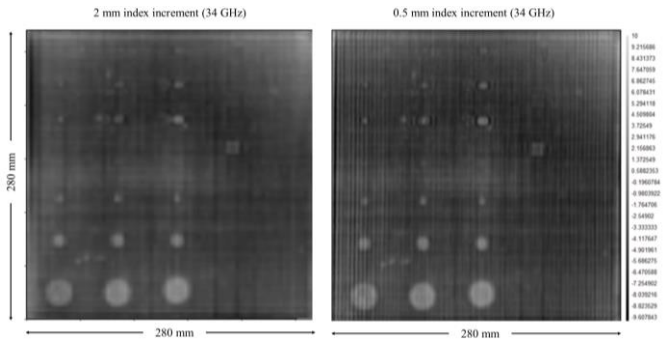

Figure 7. Inspection results for RDA2a at index increments of 2 and 0.5 mm (34 GHz)

Excerpt from ISBN 978-3-00-053387-7

4.3. Effect of RDA backing material

Fig. 8 shows the Channel C voltage signals at 34 GHz for an index increment of 0.5 mm for RDA5 scanned with two different backing materials: a thick glass plate and a sheet of mirror finish stainless steel. Detection of the artificial delaminations was in general clearer for inspections undertaken with the glass plate but the indications for back-face drilled holes (individual and array) were much clearer for inspections carried out using a steel backing plate. This was due to increased local reflections of the higher amplitude reflected signal around the hole edges. However, the amplitude of the striations at the edges and across the width of the RDAs were stronger and masked some of the smaller defects.

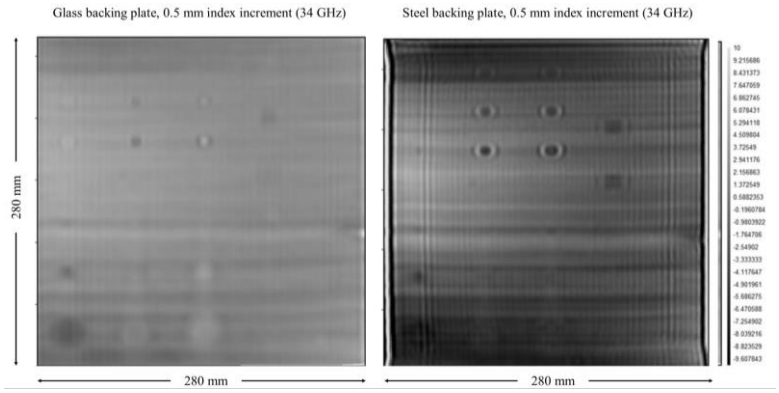

Figure 8. Inspection results for RDA5 with glass and steel backing plates (index 0.5 mm; 34 GHz)

4.4. Comparison of experimental and simulated results

Simulations were initially undertaken using estimated isotropic dielectric properties and models were subsequently re-run using the measured anisotropic dielectric properties. The Channel C inspection data in Fig. 9 showed that there were only very small differences in the simulation results, due to the small differences in directional dielectric properties caused by material anisotropy. Figures 10 shows the comparison between a simulated and experimental inspection scan for RDA5. The agreement was very good for both the drilled holes and delamination defects modelled.

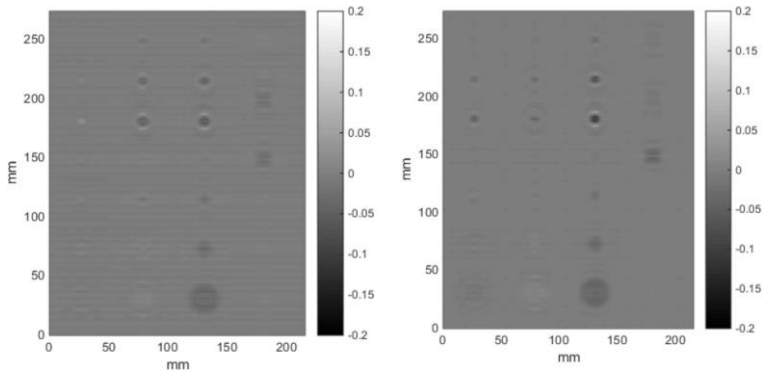

Figure 9. Simulation results for RDA2a (24 GHz, 2 mm index): isotropic (left) and anisotropic (right)

Excerpt from ISBN 978-3-00-053387-7

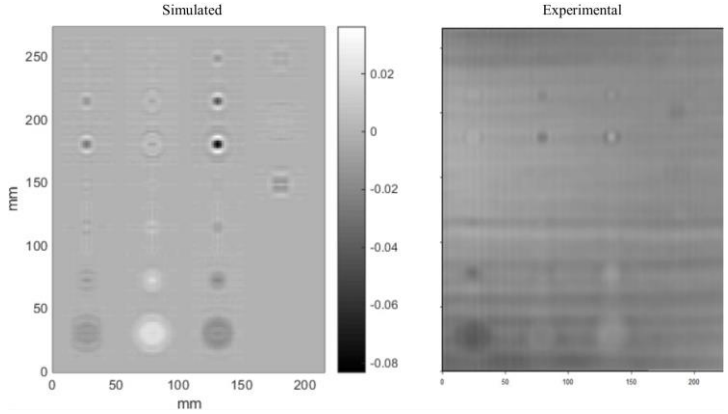

Figure 10. Comparison between simulated and experimental scans for RDA5 (24 GHz, 2 mm index)

5. Conclusions

Microwave inspection has been shown to offer good detection capability for all defect types other than regions of in-plane misalignment, with simulated and experimental results in excellent agreement. The modelling showed that striations observed in experimental scans at small index increments were due to superposition of lateral standing waves within the RDAs. The differences in isotropic and anisotropic simulations were negligible for the materials studied. The work has shown that the modelled changes in the local dielectric properties of the target induced by defects should enable the theoretical determination of probability of detection (POD) curves for microwave inspection data.

Acknowledgments

This work was funded by the ENG57 VITCEA project within the Energy 2013 call of the European Metrology Research Programme funded by EURAMET.

References

[1] ENG57 VITCEA – Validated inspection Techniques for Composites in Energy Applications. http://projects.npl.co.uk/vitcea EMRP Project.
[2] ASTM E2580 - 12 Standard Practice for Ultrasonic Testing of Flat Panel Composites and Sandwich Core Materials Used in Aerospace Applications.
[3] ASTM E2581 - 07 Standard Practice for Shearography of Polymer Matrix Composites, Sandwich Core Materials and Filament-Wound Pressure Vessels in Aerospace Applications.
[4] ASTM E2582 - 07 Standard Practice for Infrared Flash Thermography of Composite Panels and Repair Patches Used in Aerospace Applications.
[5] NPL working draft V.02 - Fibre-reinforced plastics - Ultrasonic C-scan inspection of composite structures: Part 3 - Preparation of reference defects and reference panels.
[6] Broughton, W. R., Lodeiro, M. J. and Sims, G. D., "Validation of Procedures for Ultrasonic C-Scan Inspection of PMCs: UK Round-Robin", NPL Report CMMT(A) 179, 1999.
[7] ASTM D5568 Standard Test Method for Measuring Relative Complex Permittivity and Relative Magnetic Permeability of Solid Materials at Microwave Frequencies Using Waveguide.
[8] Lynch, A. C., Evans, S. and Clarke, R.N., "The numerical relationship between permittivity and loss tangent", EMMA – Club, Technical Note No. 1, April 1998.

Excerpt from ISBN 978-3-00-053387-7